The instability of a liquid layer heated from the side when the upper surface is open to air

C. De Saedeleer, A. Garcimartin,[a] G. Chavepeyer, and J. K. Platten
University of Mons-Hainaut, B-7000 Mons, Belgium

G. Lebon
Université de Liège, B-4000 Liège, Belgium

(Received 31 October 1994; accepted 30 November 1995)

When a liquid layer is heated from the side, a monocellular flow develops immediately, no matter how small the temperature difference is. If the temperature gradient between the side walls is increased, this flow becomes unstable. Laser Doppler velocimetry measurements are reported here in an attempt to describe the main features of both the basic flow and the instability modes. It is found that before the appearance of traveling waves (the most dangerous mode as predicted by the theory), stable rolls with their axes perpendicular to the temperature gradient, span over the whole liquid layer, starting from the hot side, even if the aspect ratio (the length of the layer divided by its thickness) is very high. This unexpected situation modifies the basic flow. A further increase of the temperature gradient leads to the appearance of a time periodic motion. © *1996 American Institute of Physics.* [S1070-6631(96)01803-7]

I. INTRODUCTION

Several technically interesting situations, such as the manufacturing of crystals following the floating zone method or laser welding, involve a liquid layer with a free surface and a horizontal temperature gradient. The situation is also interesting from the point of view of the dynamics that can show up when the flow becomes unstable. Theoretical approaches are available for infinite horizontal liquid layers,[1,2] but to our knowledge, no experimental effort has been made till now to verify the extent to which the theory is valid and its range of applicability. This prompted us to carry out the present work. Before describing our results, it is therefore useful to give a brief summary of the picture provided by the theory.

There is no threshold for the onset of convective motion in a liquid layer when it is heated from one side. A so-called return flow appears as soon as a temperature difference is established between the lateral walls of the bounding container. Two mechanisms set the fluid into motion: buoyancy, that makes the fluid go up near the hot wall and down near the cold wall, and the Marangoni effect, which generates a surface fluid motion towards the cold side due to surface tension variation with temperature (we only consider the standard situation of a linear decrease of surface tension with temperature). A nondimensional number can be defined for each force: the Rayleigh number $\mathrm{Ra}=g\alpha\nabla T d^4/\kappa\nu$, and the Marangoni number $\mathrm{Ma}=-\gamma\nabla T d^2/\kappa\nu\rho$, respectively. Here, g stands for the gravity, α for the thermal expansion coefficient, ∇T for the temperature gradient, d is the layer depth, κ is the thermal diffusivity, ν is the kinematic viscosity, γ is the linear coefficient of the surface tension variation with temperature, and ρ is the density. The dynamic Bond number $\mathrm{Bd}=\mathrm{Ma}/\mathrm{Ra}$ gives their relative strength. As Ra depends on the fourth power of the layer thickness, d and Ma is proportional to the square of d, buoyancy effects are important for deep layers, while the Marangoni effect is dominant for shallow layers. One additional nondimensional number characterizes the fluid properties: the Prandtl number $\mathrm{Pr}=\nu/\kappa$. Under the assumption of a constant horizontal temperature gradient, an analytical expression for the velocity and the temperature profiles far from the lateral walls that takes into account both buoyancy and surface tension contributions can be found:[3]

$$V_x(Z)=U^*\left[\frac{Z^3}{6}-\frac{(1-3k)}{8}Z^2-\frac{(1-k)}{4}Z+\frac{(1-3k)}{24}\right], \tag{1}$$

where Z is the vertical nondimensional coordinate ($Z=2z/d-1$ such that $-1\leqslant Z\leqslant+1$), k is proportional to the dynamic Bond number ($k=\gamma/\rho\alpha g(d/2)^2$) and U^* is a reference velocity ($U^*=\partial T/\partial x\, g\alpha(d/2)^3/\nu$). The choice of coordinates is the following: z is the vertical coordinate, x is the horizontal coordinate pointing along the temperature gradient, and y is perpendicular to both x and z (see Fig. 1). Note that the form of this profile is independent of the temperature gradient and of the Pr number.

Let us mention here that the basic velocity profile was derived by Kirdyashkin[4] three years before the paper in Ref. 3. In Ref. 4, the shape of the velocity profile is exactly the same as given in Ref. 3, but the amplitude is quite different and given by $[30/(3-5k)\mathrm{Ra}^*]^{1/2}$, where Ra* is a modified Rayleigh number. This is a manifestly incorrect result, since a correct theory should not rule out the case $k\geqslant 3/5$.

An alternate form of the basic velocity profile (1) is

$$V_x(Z)=U^*\left[\frac{Z^3}{6}-\frac{Z^2}{8}-\frac{Z}{4}+\frac{1}{24}\right]+U^*k\left[\frac{3}{8}Z^2+\frac{Z}{4}-\frac{1}{8}\right] \tag{2}$$

or in a dimensionless form, using the definition of U^* and k:

[a]Permanent address: Department de Fisica y Matematica, Fac. de Ciencias, Universite de Navarra, E-31080 Pamplona, Spain.

 1070-6631/96/8(3)/670/7/$10.00

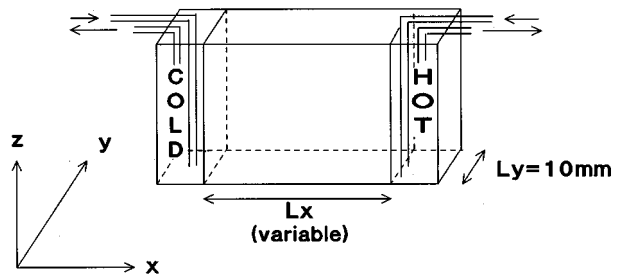

FIG. 1. Sketch of the experimental cell.

$$\tilde{V}_x(Z)=\frac{V_x(Z)}{(\kappa/d)}=\frac{\mathrm{Ra}}{8}\left[\frac{Z^3}{6}-\frac{Z^2}{8}-\frac{Z}{4}+\frac{1}{24}\right]-\frac{\mathrm{Ma}}{2}\left[\frac{3}{8}Z^2+\frac{Z}{4}-\frac{1}{8}\right]. \tag{3}$$

Thus the basic velocity profile contains two separate contributions: one proportional to the Rayleigh number and related to buoyancy forces, the second to the Marangoni number, or to surface tension forces.

Regarding the temperature distribution, one has to solve the heat equation

$$V_x(z)\,\frac{\partial T}{\partial x}=\kappa\nabla^2 T \tag{4}$$

with the assumption $V_z=0$, only valid in an horizontal infinite layer. The solution of (4) is simply

$$T(x,\ z)=g(z)+Ax, \tag{5}$$

where A is the constant applied horizontal temperature gradient

$$A=\frac{\partial T}{\partial x}=\boldsymbol{\nabla} T=c^{st}. \tag{6}$$

The function $g(z)$ is obtained by integrating twice

$$\frac{\partial^2 g}{\partial z^2}=\frac{A}{\kappa}\,V_x(z) \tag{7}$$

and is thus a polynomial of the fifth degree. Its detailed expression, not given here, depends on both Ra and Ma. But the main point is that the horizontal applied temperature gradient A is constant, independent of elevation z and of the relative contribution of surface tension and buoyancy forces. In some sense, it is the control parameter, which needs to be measured in any careful experiment. But since it is independent of elevation z, we may measure this temperature gradient where we like, namely along the surface for facility reasons. And this does not mean at all that the velocity profile, when we put in U^* the measured *surface* temperature gradient, is behaving as it felt only surface effects: we could equally well put in U^* the temperature gradient taken at any elevation z since it is constant. This point sometimes escapes to the attention of the reader.

Smith and Davis[1] assume Ra$\rightarrow$0, i.e., a zero gravity condition (therefore $k\rightarrow\infty$), as a starting point for their stability analysis. The velocity profile is thus quadratic in that case. Under this stringent hypothesis, it was found that the so-called surface waves and hydrothermal waves were the most dangerous modes, the former being just a shear instability, and the latter a more complex interplay between the temperature and velocity fields.

A more general approach was carried out by Parmentier, Regnier, and Lebon.[2] They take into account both the buoyancy and the thermocapillary effects, and found the instability curve in a Ma–Ra space, as well as the speed and the wave number for the unstable waves.

II. DISCUSSION OF THE EXPERIMENTAL RESULTS

Our experiments were designed to be compared with those theoretical predictions. The liquid we use is decane (Pr=15) for which numerical results are available.[5] Because of the small vapour pressure of decane, the thickness of the layer remains constant even after long experimental runs. The container where convection takes place, is made of quartz, with two copper boxes at the ends that are kept at a constant temperature by circulating water (see Fig. 1). The free distance between the copper blocks is at most 74 mm but can be made smaller by moving the two copper boxes closer together, and the width of the channel is 10 mm in all cases. Two thermostatic baths provide the water at a temperature stabilized within ± 0.02 °C. The room where the experiments where performed was kept at a constant temperature of about 20–21 °C. The temperature difference between the lateral walls was chosen so that the mean was about the room temperature, except in the case of large temperature gradients, for which the lowest temperature T_{cold} was fixed to 14 °C to avoid condensation on the front and back walls. Moreover, as quartz is a relatively good thermal conductor, we wrapped the cell with insulating foam except where optical access is needed. Care was taken to avoid pollution of the liquid, which would drastically change its surface tension. In the experimental runs, we used indistinctly two quartz cells of the same dimensions, to be sure that none of the features reported were due to small imperfections of the container. A standard TSI laser-Doppler velocimeter (LDV) was used. The laser source is a 35 mW He–Ne laser, and the photodetector signal is sent to a HP 3561-A Dynamic Signal Analyser which performs the signal analysis with a FFT algorithm. The signal analyser is in turn connected to a PC via GPIB. In order to move the cell for obtaining velocity profiles, it is placed on a computer-controlled 3-axis translation stage, with stepping motors having a 10 μm step. The depth of the layer was measured using the magnifying lenses of the photodetector optical arrangement; uncertainties in the layer thickness amount to 0.1 mm, approximately.

We begin by comparing the experimental basic flow with the theoretical expression (1) for different depths and lengths of the layer. In order to do this comparison, we need to know all the parameters that characterize the fluid used, decane. We measured the surface tension temperature dependence ($-9.53\cdot10^{-5}$ N/m/K), the kinematic viscosity ($1.25\cdot10^{-6}$ m^2/s) and the thermal expansion coefficient ($1.076\cdot10^{-3}$ K^{-1}), values which agreed with those found in the literature.[6] So with these measured parameters, we calculated the theoretical values of the horizontal velocity using the expression (1) and supposing that the temperature gradient can be ap-

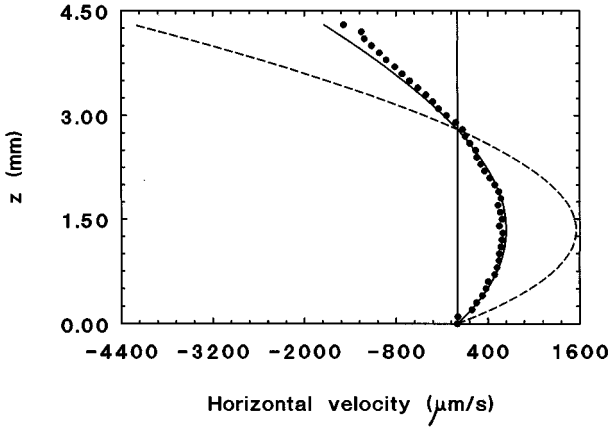

FIG. 2. Horizontal velocity profile $V_x(z)$ for $L_x=50$ mm, $d=4.3$ mm, and $\Delta T=1.7$ °C between the thermostatic baths. ● experimental LDV measurements; --- analytical curve with $\nabla T=\Delta T/L_x$; — analytical curve with ∇T really measured.

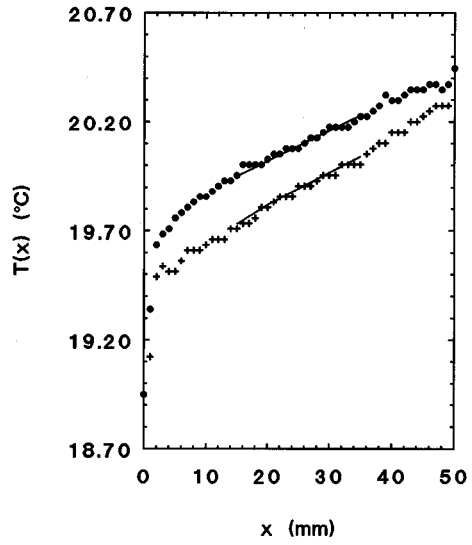

FIG. 3. Temperature profiles $T(x)$ for $L_x=50$ mm and $d=4.3$ mm and $\Delta T=1.7$ °C between the thermostatic baths. ● taken on the surface $z=d$, + taken in the bulk $z=d/2$.

proximated by $\nabla T=\Delta T/L_x$, where ΔT is the temperature difference between hot and cold walls and L_x the length of the container. The so made predictions are very different from the experimental values (see Fig. 2). Then we measured the surface temperature along the length of the container (the x axis). For this we used thermocouples K (chromel-Alumel) with an experimental error of about 1 μV (0.02 °C). We immerse the thermocouple just below the surface near the cold side, perform the measurement, and then take it out of the decane and reimmerse it nearer the hot one (with a step of 1 mm). This procedure is used to avoid any perturbation due to the displacement of the thermocouple in the decane. This surface temperature profile is given in Fig. 3. So we observed that the overall horizontal temperature gradient imposed by the two copper boxes was more than two times greater than the gradient really suffered at the middle of the layer, where we performed our measurements of the velocity profile. To be sure that the horizontal temperature gradient is independent of elevation, we measured (in a few runs) this gradient not only in the surface, but also at mid-height and near the bottom. Of course measuring the temperature gradient in the bulk is a disturbing process due to the displacement of the thermocouple. Anyway, we give in Fig. 3, a comparison of the two temperature profiles taken at $z=d$ (or $Z=1$) and at $z=d/2$ (or $Z=0$). We have found at $x=25$ mm (in the middle of the cavity)

$$\left(\frac{\partial T}{\partial x}\right)_{z=d} = 13.8 \pm 0.9 \ \text{K/m},$$

$$\left(\frac{\partial T}{\partial x}\right)_{z=d/2} = 15.4 \pm 1.0 \ \text{K/m}.$$

They agree with each other in the limit of the given experimental errors. In the remainder of this paper, we shall always take what we hope to be the less disturbed value, i.e., the surface temperature gradient. Next we recalculated the ''real'' theoretical values of the horizontal velocity with this *measured* temperature gradient and it can be seen in Fig. 2 that the theoretical curve predicted by the expression (1) used together with the experimental temperature gradient, fitted the experimental values very well. The standard deviation between theoretical and experimental values for a layer of 4.3 mm depth and 50 mm length (see Fig. 2), is ~100 μm/s; the experimental error is estimated to be approximately 30 μm/s.

Such a good agreement is also obtained for different fluid depths, changing the relationship between Ra and Ma.

We checked that there is a portion of the cell where the horizontal velocity is approximately constant. For example, we can see in Fig. 4 (for another experimental run performed with a layer of 74 mm length and 2.5 mm depth) that the velocity (measured at 0.9 mm height) is constant for 25 mm $<x<$45 mm. Since the temperature gradient is larger near

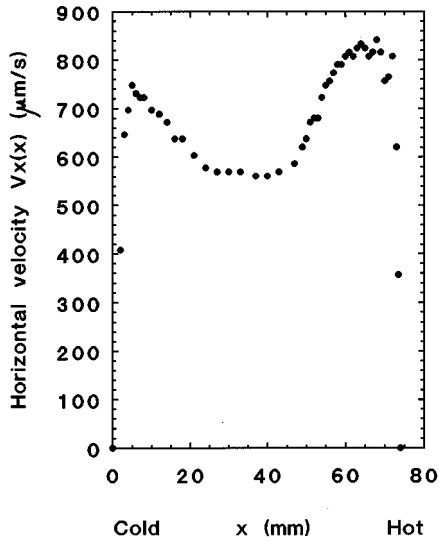

FIG. 4. Experimental LDV measurements of the horizontal velocity $V_x(x)$ at $z=0.9$ mm for $L_x=74$ mm, $d=2.5$ mm, and $\Delta T=4.1$ °C between the thermostatic baths.

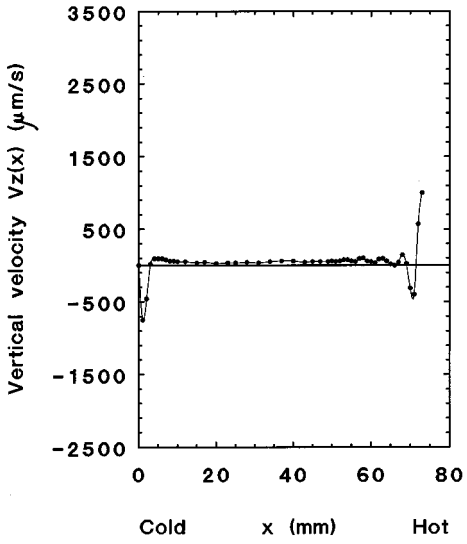

FIG. 5. Vertical velocity $V_z(x)$, experimental LDV measurements at $z=2.4$ mm for $L_x=74$ mm, $d=3.2$ mm, and $\Delta T=4.05$ °C between the thermostatic baths.

the ends, the horizontal velocity there is correspondingly larger. Near the walls, V_x vanishes, and in the central part (excluding 25 mm at each side, say) it is approximately constant. The existence of this zone means that we can consider the velocity profile there, at this stage, as being the same as in an infinite layer.

Experiments were made for different layer lengths: 30, 50, 74 mm and heights $d=4.3$ mm and $d=4.7$ mm (so giving aspect ratios in the range 7–17) and keeping the temperature gradient constant for the three lengths thus changing appropriately $(T_{\text{hot}}-T_{\text{cold}})$. We have observed that, for these three lengths, the theoretical values fitted very well the experiments for small gradients. We can see that the experimental velocity profiles performed here in decane are similar to those observed by Villers and Platten in acetone with an aspect ratio of about 10 (Ref. 7) but in this last paper the comparison with a theoretical formulation was not given because the temperature profile was not measured and only a comparison with a numerical simulation was realized. The missing key to compare experiments and theory was the *real* temperature gradient, as demonstrated here for decane. The velocity profile is also correctly reproduced by numerical calculations using finite differences to discretize the Navier–Stokes and energy equations.[8]

Near the hot wall (at $x\approx 70$ mm) there are small irregularities, but it is in the variation of the vertical velocity component with x, $V_z(x)$, as we will show below, that these irregularities can be fully appreciated. In our geometry, the growth of any transverse disturbances (if present) is probably suppressed, and we have therefore concentrated on measuring $V_x(z)$ and $V_z(x)$ when looking for disturbances.

In Fig. 5 we show a profile of $V_z(x)$ *at small temperature gradient* (both Ra and Ma small). The measurements show that the basic flow is almost one dimensional in the middle of the cell. We have nevertheless observed that a small vertical velocity component is present. The values for this residual vertical velocity V_z are typically of the order of 50 μm/s, which is just bigger than the smallest detectable velocity above experimental error. This upward flow could be the result of subtle surface tension variation due to the influence of the lateral walls. As this value is two orders of magnitude below the surface velocities we will be dealing with, we will neglect it in the following. Of course, there is vertical motion near the cold and the hot walls, even for small temperature differences. Besides, one can notice that near the hot wall several rolls of small amplitude are present, but one can conclude that the basic flow at the middle of the cell is in good agreement with the theory.

Let us now comment here on possible three dimensional effects. If present, they are certainly due to: (i) the nonslip at the sidewalls and (ii) a possible small temperature gradient in the y direction producing a subtle surface tension gradient in this direction as already said in the previous paragraph. We checked that the velocity profiles along the y direction, $V_z(y)$ and $V_x(y)$ are almost constant in the y direction, except in the boundary layers confined approximately 2 mm from the lateral walls (front and back walls). In the central part of the cell velocity profiles were taken on the axis and 1.5 mm apart from the axis and no difference was appreciated. We feel it is not worth giving these profiles here. The temperature gradient in the y direction, certainly small since the lateral walls were wrapped with insulating foam except where optical access is needed, could lead to a secondary thermocapillary flow. This possibly takes the form of two longitudinal rolls, with their axes aligned parallel to the temperature gradient and superimposed on the main thermocapillary vortex. This is consistent with the small upward velocity of about 50 μm/s measured near the cell axis (see Fig. 5). This is to be compared with the typical values of several millimeters/second of the main flow. Therefore, such three-dimensional effects seem to be small with respect to the main flow and will be ignored in the following. Also, the transverse component of the velocity Vy is not accessible to laser-Doppler measurements, since only velocity components in a plane perpendicular to the optical axis (the x-z plane) can be measured. It is however clear that additional work is needed to further elucidate three-dimensional effects, but this is outside the scope of this paper, since we focus only on the stability of the main thermocapillary vortex. There are, however, two papers studying numerically the arising of three-dimensional effects in thermocapillary convection alone (absence of gravity)[9] and in buoyant thermocapillary convection.[10] These authors paid attention to three-dimensional effects that are induced by the presence of sidewalls, describing several secondary vortices (in particular, see Fig. 4 of Ref. 9). However the aspect ratios are totally different: a cubic container in Ref. 9 and 1 (height), 1.4 (width), and 1.7 (length) in Ref. 10. In our case, the aspect ratios are approximately 1, 3, and 20. Anyway, if we follow the results obtained by Mundrane and Zebib,[10] our flow is not expected to become three dimensional. In fact, they state that for $\text{Ma}=2.93\times 10^3$ the flow is two dimensional, and three dimensional for $\text{Ma}=1.95\times 10^5$. In our experiments, Ma is well below that figure: typically around 1×10^3. Three-dimensional effects found for larger Marangoni numbers (two orders of magnitude bigger) involve vertical velocities

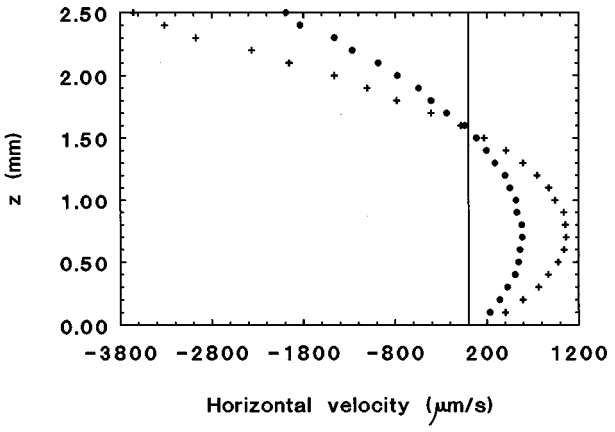

FIG. 6. Horizontal velocity $V_x(z)$, experimental LDV measurements for $L_x=74$ mm and $d=2.5$ mm and ● $\Delta T=4$ °C; + $\Delta T=8$ °C between the thermostatic baths.

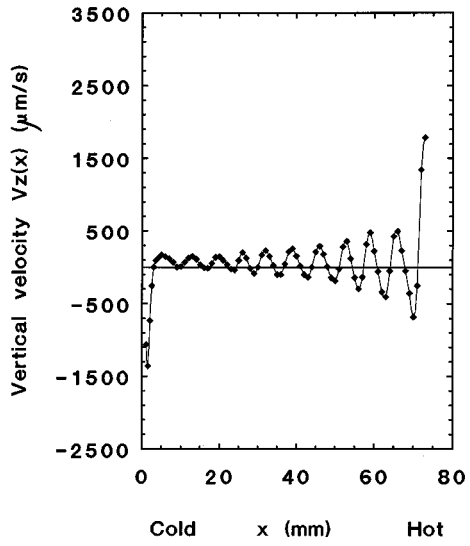

FIG. 7. Vertical velocity $V_z(x)$, experimental LDV measurements at $z=2.4$ mm for $L_x=74$ mm, $d=3.2$ mm, and $\Delta T=8.0$ °C between the thermostatic baths.

near the center of the cell of about 0.4 mm/s, while we found 0.05 mm/s. Therefore, we are confident that our experiment is basically two dimensional, at least near the center of the cell.

Next, we increased the temperature gradient, in an attempt to verify the critical curve calculated by Lebon and his coworkers for Pr=15.[5] We checked both V_z and V_x when searching for instabilities. The *shape* of the profiles $V_x(z)$ do not change significantly when increasing the temperature difference (see Fig. 6). By the way, let us mention that, since the applied temperature gradients differ by a factor of 2, one could expect from Eq. (1) that the two curves also differ by the same factor. This is not the case. Indeed, at $\Delta T=8$ °C, the profile do not obey Eq. (1) because the applied temperature gradient is too large and we are in the instability domain where Eq. (1) is invalid (see below).

The scenario for instability found in virtually every run for $V_z(x)$ was totally different from what we expected. Before reaching any oscillatory instability, the small rolls found in Fig. 5 near the hot end are seen to grow and to spread over the whole cell (Fig. 7). This can be linked to a diffusion process, the amplitude exponentially decaying with distance from the hot end. Eventually, the rolls invade all the cell and a constant amplitude is reached (Fig. 8). This kind of rolls has been observed before.[7,11,12] In Refs. 7 and 11 little attention was paid to these rolls, either because they were regarded as a transient state of small amplitude compared to the main flow, or because it was thought that small aspect ratio was causing rolls to appear. In Ref. 12 more detailed observations are provided. This pattern merits a deeper discussion, and we focus here only on the birth and development of these rolls.

We have checked that the rolls are stable both in space and time (after a transient of some minutes typically). It is also worth noticing that we have found that they develop for every situation we have explored, from $d=2.5$ mm to $d=3.6$ mm (which means a decrease in the dynamic Bond number by 200%). The aspect ratio (the length divided by the layer thickness) ranges from about 20 to 30. In other pattern-forming systems (such as Rayleigh–Bénard convection, for example) this could be considered as an infinite container, and lateral boundary conditions could be ignored at least as far as the critical point $\mathrm{Ra}^{\mathrm{crit}}$ is concerned (the standard critical value $\mathrm{Ra}^{\mathrm{crit}}\approx 1708$ is already reached for an aspect ratio of the order of 6). This is certainly due to the fact that in Rayleigh–Benard convection the basic state, which is the rest state, is observed everywhere including near the boundaries. This is not the case here, since the basic state described by Eq. (1) is only observed in the center of the cavity, not near the end walls. In our case, the rolls always end up by invading all the cell, starting from the hot wall. If the depth is varied only the wavelength is observed to change, but the scenario remains exactly the same. One could conceivably think of increasing the aspect ratio in order to observe traveling waves at threshold. But one has also to increase the temperature difference between the walls by the same amount if one wants to establish the same temperature gradient. This means that a higher temperature gradient will be present near the hot wall, and the rolls would eventually diffuse throughout the cell as well. So it is our belief that it is not possible to reach an aspect ratio that one can regard as infinite. In other words, lateral boundary conditions can never be neglected when heating from one side. The question arising now is: Is it, however, possible to ignore the existence of these rolls because of their small amplitude? This is not found to be the case. Typical vertical velocities are about 0.5 mm/s (see Fig. 8), and the velocity of the basic flow is of the order of a few millimeters/second. So rolls cannot be ignored or regarded as a small perturbation. They are to be taken into account in any realistic theoretical or numerical description, and they are by no means spurious.

We have observed that a further increase of the temperature gradient leads to the appearance of a time periodic flow pattern. Travelling waves have been characterized for an intermediate Pr number and described in a phenomenological fashion for a high Pr number fluid.[13] Therefore, we have not devoted our effort to study time dependent patterns, although

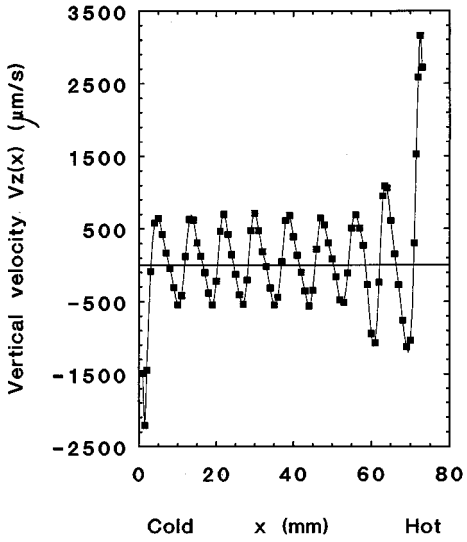

FIG. 8. Vertical velocity $V_z(x)$, experimental LDV measurements at $z=2.4$ mm for $L_x=74$ mm and $d=3.2$ mm and $\Delta T=11.9$ °C between the thermostatic baths.

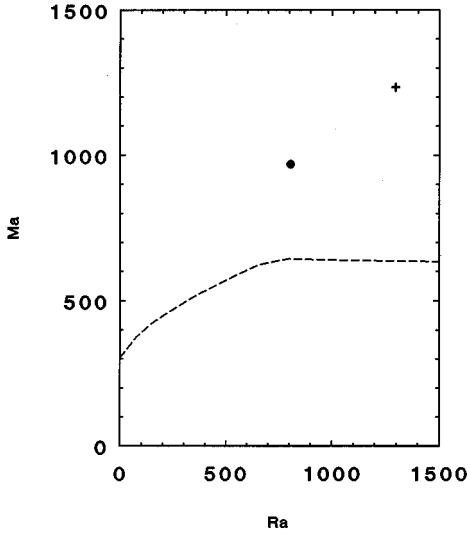

FIG. 10. Stability diagram. --- critical curve from linear stability analysis;[5] ● oscillations for $L_x=74$ mm, $d=3.2$ mm, $\Delta T=15.9$ °C; + oscillations for $L_x=74$ mm, $d=3.6$ mm, $\Delta T=16$ °C.

there are some interesting aspects that could be the subject of future work. Moreover, laser Doppler velocimetry is not very well suited to perform measurements of a rapidly changing velocity pattern. We have nevertheless been able to check that the period (about 2 s) is in good agreement with previous observations, and that the horizontal velocity oscillates with the same period as that of the vertical component. At the expense of losing accuracy, one can track at a given point the velocity with the LDV at a sampling rate of about 12 measurements/s (see Fig. 9) without a large amount of seeding and observe that the amplitude of the velocity oscillations grows with the temperature difference, although the period remains approximately constant from the very onset. The two experimental points where oscillations have been observed are shown in Fig. 10, together with the critical curve calculated for Pr=15.[5]

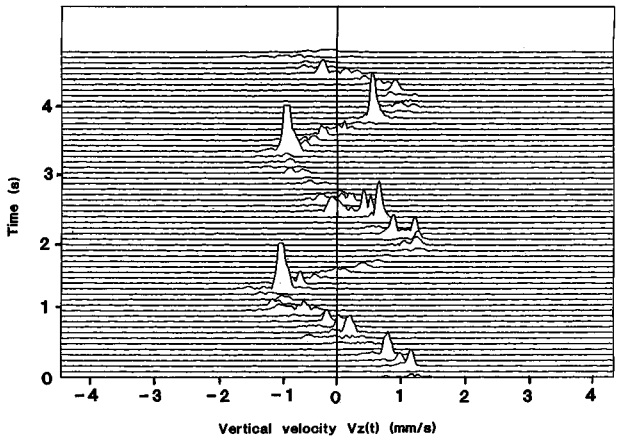

FIG. 9. Vertical velocity with time $V_z(t)$ measured at $x=5$ mm, $z=2.05$ mm for $L_x=74$ mm and $d=3.6$ mm and $\Delta T=16$ °C between the thermostatic baths.

III. CONCLUSIONS

The most important conclusion that one can extract from these experiments is, in our opinion, the fact that the boundaries have to be taken into account if one wants to properly describe the convection of a liquid layer heated from the side. No matter how big the aspect ratio is, rolls appear transversally to the temperature gradient with a velocity smaller but not negligible when compared to the basic flow, before the appearance of oscillatory instabilities. The existence of steady transverse rolls is not predicted by the stability theory of an infinite layer.

ACKNOWLEDGMENTS

We have greatly benefited from the numerical results provided by Lebon and coworkers (University of Liège) with our fluid parameters. We also want to thank M. Bettignie and P. Smet for their technical help. This text presents research results of the Belgian programme on Interuniversity Poles of Attraction initiated by the Belgian State, Prime Minister's Office, Science Policy Programming. The scientific responsibility is assumed by its authors.

[1] M. K. Smith and S. H. Davis, "Instabilities of dynamic thermocapillary liquid layers. Part 1. Convective instabilities," J. Fluid Mech. **132**, 119 (1983).
[2] P. M. Parmentier, V. C. Regnier, and G. Lebon, "Buoyant-thermocapillary instabilities in medium-Prandtl-number fluid layers subject to a horizontal temperature gradient," Int. J. Heat Mass Transfer **36**, 2417 (1993).
[3] D. Villers and J. K. Platten, "Separation of Marangoni convection from gravitational convection in earth experiments," Phys. Chem. Hydrodyn. **8**, 173 (1987).
[4] A. G. Kirdyashkin, "Thermogravitational and thermocapillary flows in a horizontal liquid layer under the conditions of a horizontal temperature gradient," Int. J. Heat Mass Transfer **27**, 1205 (1984).
[5] G. Lebon, private communication (the numerical results of Ref. 2 were recalculated for the experimental case Pr=15).
[6] N. B. Vargaftik, *Handbook of Physical Properties of Liquids and Gases*, 2nd ed. (Springer-Verlag, Berlin, 1975).
[7] D. Villers and J. K. Platten, "Coupled buoyancy and Marangoni convec-

tion in acetone: experiments and comparison with numerical simulations,'' J. Fluid Mech. **234**, 487 (1992).
[8]C. De Saedeleer, G. Chavepeyer, and J. K. Platten, ''A 2D computer simulation of thermocapillary convection in finite layers,'' in *Proceeding of the 2nd International Thermal Energy Congress*, Agadir, edited by E. Bilgen, A. Mir, T. M. Nguyen, and P. Vasseur (1995), Vol. 2, p. 814.
[9]V. Sass, H. C. Kuhlmann, and H. J. Ruth, ''Investigation of 3D thermocapillary convection in a cubic container by a multi-grid method,'' Int. J. Heat Mass Transfer **39**, 603 (1996).
[10]M. Mundrane and H. Zebib, ''Two- and three-dimensional buoyant thermocapillary convection,'' Phys. Fluids. A **5**, 810 (1993).
[11]A. B. Ezersky, A. Garcimartin, T. Burguete, H. L. Mancini, and C. Pérez-Garcia, ''Hydrothermal waves in Marangoni convection in a cylindrical container,'' Phys. Rev. E **47**, 1126 (1993).
[12]D. Schwabe, U. Möller, J. Schneider, and A. Scharmann, ''Instabilities of shallow dynamic thermocapillary liquid layers,'' Phys. Fluids A **11**, 2368 (1992).
[13]A. B. Ezersky, A. Garcimartin, H. L. Mancini, and C. Pérez-Garcia, ''Spatiotemporal structure of hydrothermal waves in Marangoni convection,'' Phys. Rev. E **48**, 4414 (1993).